

Article

Reverse Osmosis with Intermediate Chemical Demineralization: Scale Inhibitor Selection, Degradation, and Seeded Precipitation

Shichang Xu ¹, Ping Wang ¹, Lixin Xie ^{1,*}, Yawei Du ² and Wen Zhang ^{1,*} 

¹ Tianjin Key Laboratory of Membrane Science and Desalination Technology, State Key Laboratory of Chemical Engineering, School of Chemical Engineering and Technology, Tianjin University, Tianjin 300350, China; xu_sc1@tju.edu.cn (S.X.); pingwang_971213@tju.edu.cn (P.W.)

² School of Chemical Engineering and Technology, Hebei University of Technology, Tianjin 300401, China; sonicduyawei001@126.com

* Correspondence: xie_lixin@tju.edu.cn (L.X.); zhang_wen@tju.edu.cn (W.Z.)

Abstract: Two-stage reverse osmosis (RO) processes with intermediate concentrate demineralization (ICD) provide an efficient strategy to treat brines with high CaSO₄ contents and reduce concentrate discharge. In this paper, an SRO concentrate is treated using ICD to remove CaSO₄ and then mixed with a PRO concentrate for further desalination in SRO, thereby reducing the discharge of the concentrate. We investigate the selection and degradation of scale inhibitors, as well as seeded precipitation in the two-stage RO process with ICD, to achieve a high water recovery rate. A scale inhibitor is added to restrain CaSO₄ crystallization on the membrane surface, and the optimized scale inhibitor, RO-400, is found to inhibit calcium sulfate scaling effectively across a wide range of the saturation index of gypsum (SI_g) from 2.3 to 6. Under the optimized parameters of 40 W UV light and 70 mg/L H₂O₂, UV/H₂O₂ can degrade RO-400 completely in 15 min to destroy the scale inhibitor in the SRO concentrate. After scale inhibitor degradation, the SRO concentrate is desaturated by seeded precipitation, and the reaction degree of CaSO₄ reaches 97.12%, leading to a concentrate with a low SI_g (1.07) for cyclic desalination. Three UVD-GSP cycle tests show that the reused gypsum seeds can also ensure the effect of the CaSO₄ precipitation process. This paper provides a combined UVD-GSP strategy in two-stage RO processes to improve the water recovery rate for CaSO₄-contained concentrate.

Keywords: RO concentrate; CaSO₄; scale inhibitor; UV/H₂O₂ degradation; seeded precipitation



Citation: Xu, S.; Wang, P.; Xie, L.; Du, Y.; Zhang, W. Reverse Osmosis with Intermediate Chemical Demineralization: Scale Inhibitor Selection, Degradation, and Seeded Precipitation. *Molecules* **2024**, *29*, 2163. <https://doi.org/10.3390/molecules29102163>

Academic Editor: Shaojun Yuan

Received: 28 March 2024

Revised: 25 April 2024

Accepted: 2 May 2024

Published: 7 May 2024



Copyright: © 2024 by the authors. Licensee MDPI, Basel, Switzerland. This article is an open access article distributed under the terms and conditions of the Creative Commons Attribution (CC BY) license (<https://creativecommons.org/licenses/by/4.0/>).

1. Introduction

Reverse osmosis (RO) has been widely used in brine desalination because of its simple process and low energy consumption [1–3]. After brine treatment, RO produces a large amount of salt-containing concentrate with a complex composition [4,5]. Secondary reverse osmosis (SRO) can further treat the salt-containing concentrate to reduce the amount of high-concentration brine. The two-stage RO process integrating RO desalination with intermediate concentrate demineralization (ICD) is one of the promising strategies to overcome the recovery limitation caused by mineral scaling during RO desalination [6–11]. ICD can reduce the concentration of calcium sulfate in the RO concentrate, allowing it to be further desalted in a subsequent SRO process [6,12].

In the concentrated water of primary reverse osmosis (PRO), there is usually a high concentration of calcium sulfate (CaSO₄). For example, the saturation index of CaSO₄ (SI_g) can reach up to 0.7 in the concentrated water of PRO for the treatment of brine in the coal chemical industry [13]. Because of concentration polarization (CP) [14], the SI_g on the RO membrane surface can exceed 4 when the SRO recovery rate is 70% [15]. Hence, a scale inhibitor is necessary before SRO to avoid mineral salt scaling on the surface of the SRO membrane [16–18]. After SRO, the scale inhibitors in the SRO concentrate need to be destroyed to precipitate CaSO₄ [17,19]. Accordingly, we propose the following two-stage

RO process with ICD to treat brines (Figure 1), where the SRO concentrate is treated with ICD to remove CaSO_4 and then mixed with the PRO concentrate for further desalination in SRO.

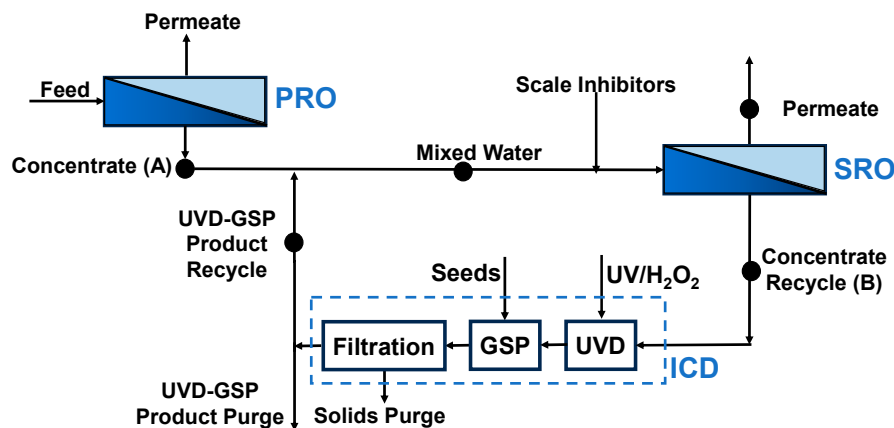


Figure 1. Schematic diagram of the two-stage RO process with ICD (UVD-GSP).

In the ICD process, gypsum seeded precipitation (GSP) has been used to remove CaSO_4 [7,20,21]. Before seeded precipitation, a scale inhibitor should be removed because of its inhibiting effect on the crystallization process of CaSO_4 [17,19]. Coagulation is a conventional method for removing scale inhibitors. For example, polyaluminum chloride and surfactant sodium dodecyl sulfate have been used to adsorb scale inhibitors for the formation of CaSO_4 precipitation. However, the residual product will aggravate the surface fouling of the RO membrane [22–24]. Adjusting the pH can induce the precipitation of CaCO_3 [7,20,21]. However, it is not effective for the CaSO_4 system [8]. Therefore, it is necessary to develop new methods to remove scale inhibitors before gypsum seeded precipitation.

The degradation of scale inhibitors is a promising method for removing scale inhibitors [25–27]. For example, ultraviolet-driven persulfate oxidation (UV/PS) is used to degrade scale inhibitors and promote CaCO_3 precipitation successfully [19]. However, the use of persulfate as an oxidant will introduce new impurity ions to the RO system and increase the salt content. H_2O_2 is also a common oxidant that will not introduce new impurities and salts [28,29]. Nevertheless, there are few studies on UV/ H_2O_2 in the treatment of RO concentrate with a high concentration of CaSO_4 . In addition, it is important to study the whole process of SRO to treat concentrated solutions containing high calcium sulfate. However, there are few reports about the process.

This paper systematically addresses the optimization of three components of the UVD-GSP process, which include the following: scale inhibitor selection, degradation, and seed precipitation. We investigate the inhibiting effect of different scale inhibitors on the CaSO_4 concentrate first and then develop an ICD process using UV/ H_2O_2 degradation of the scale inhibitor (UVD) and gypsum seeded precipitation (GSP) to treat the RO concentrate with a high concentration of CaSO_4 (Figure 2). Four common commercial-scale inhibitors were used to treat the CaSO_4 concentrate by static scale inhibition experiments. The effects of scale inhibitor dose, pH, and temperature were studied for the selected inhibitors. Then, the feasibility of removing scale inhibitors from RO concentrates by UVD was studied, and the removal efficiency was explored in relation to UV intensity, H_2O_2 dose, and light pretreatment time. In subsequent GSP, the effect of seed size, loading amount, and recyclability on gypsum precipitation performance was assessed and optimized to obtain a high reaction degree of CaSO_4 and a low saturation index of gypsum. This paper provides a clean and highly efficient method based on UV/ H_2O_2 to remove scale inhibitors from RO concentrates, without the introduction of impurities into the entire system. The whole process studied to treat the concentrated solution containing high calcium sulfate by SRO,

including scale inhibitor selection, degradation, and seed precipitation, can also provide guidance for actual production.

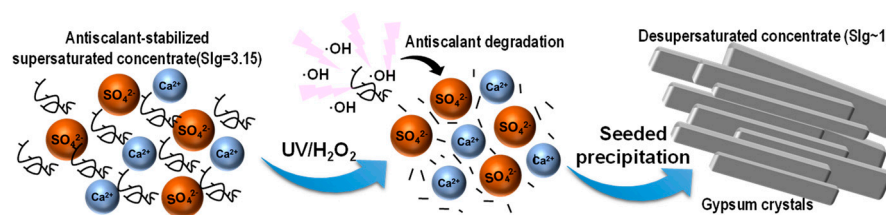


Figure 2. UVD-GSP mechanism for the removal of calcium sulfate from RO concentrates.

2. Results and Discussion

2.1. Static Scale Inhibition Experiment

We evaluated the inhibition performance of different scale inhibitors. In Figure 3a, with the gradual increase in the SIg, scaling is observed in the simulated concentrates with different scale inhibitors. The SIg values of TH-1100, SI-001, EDTMPS, and RO-400 are 3, 3.5, 4, and 6, respectively. Therefore, RO-400 has the best scale inhibition effect. Figure 3b is a digital photograph of the model concentrate after adding different scale inhibitors for 10 h when the SIg = 6.5. It can be seen that the amount of scale in the model concentrate with RO-400 is the least. SEM images of CaSO₄ precipitation are shown in Figure 3c. In the presence of TH-1100, the micro-morphology of CaSO₄ precipitation is basically the same as that without the scale inhibitor (Figure S1).

In the presence of RO-400, the crystal structure of CaSO₄ is damaged dramatically. There are only loose and broken small particles, without the original plate-like structure of CaSO₄. These small particles are easily washed away by backwashing, thereby reducing the adverse effects of CaSO₄ precipitation. Therefore, RO-400 has the best anti-CaSO₄ precipitation performance across a wide range of the SIg from 2.3 to 4. This may be due to the fact that the carboxyl group on the main chain of the polymer is an effective functional group to inhibit the formation of scale [30,31]. Therefore, in the following experiments, RO-400 was used as the optimized scale inhibitor.

The effects of dose, pH value, and temperature on scale inhibition performance were also studied for the RO-400 inhibitor. In Figure 3d, η initially increases with the increase in the RO-400 dose and then reaches 100% at the RO-400 dose of 3 ppm [32]. In Figure 3e, the scale inhibitor performs well across a wide range of pH values from 5 to 11. This pH range is basically consistent with that of industrial RO influent, indicating the high industrial application potential of RO-400. In Figure 3f, η is relatively stable in the range of 15–30 °C. However, it should be noted that when the temperature is higher than 30 °C, η may decrease because of the enhanced molecular movement, and a higher dose of RO-400 may be required to cope with this situation [33].

2.2. UVD-GSP Processes

The effects of UVD operating parameters on the performance of UVD-GSP were studied here, including UV intensity, H₂O₂ dose, and light pretreatment time (t_p) [29]. The results were compared to the contrast groups, the PBL group without RO-400 (RO-400-free), and the NBL group containing 10 ppm RO-400 but without UVD treatment (RO-400 + UVD-free). The PBL and NBL groups represent the upper and lower limits of the scale inhibitor removal effect in the UVD process, respectively.

Figure 4a demonstrates the effect of UV intensity on the UVD-GSP processes. In the UVD stage, when using a UV light of 20 W for the irradiation of 15 min, 3% of the scale inhibitor remained (Table S1). Then, 2.5 g/L (7–43 μ m) of seed crystal is added. After the 180-min GSP desaturation process, the precipitation degree of CaSO₄ reaches 87.8%, and the SIg is 1.25. The residual scale inhibitor ratio (R) gradually becomes smaller with the increase in UV intensity. When the light intensity reaches 40 W, there is no residual scale inhibitor in the UVD stage. After the 180-min GSP desaturation process, the precipitation degree

of CaSO_4 increases to 97.12%, and the SIg decreases to 1.07. The kinetic curve of CaSO_4 precipitation in this situation is very close to the curve of GSP without the scale inhibitor.

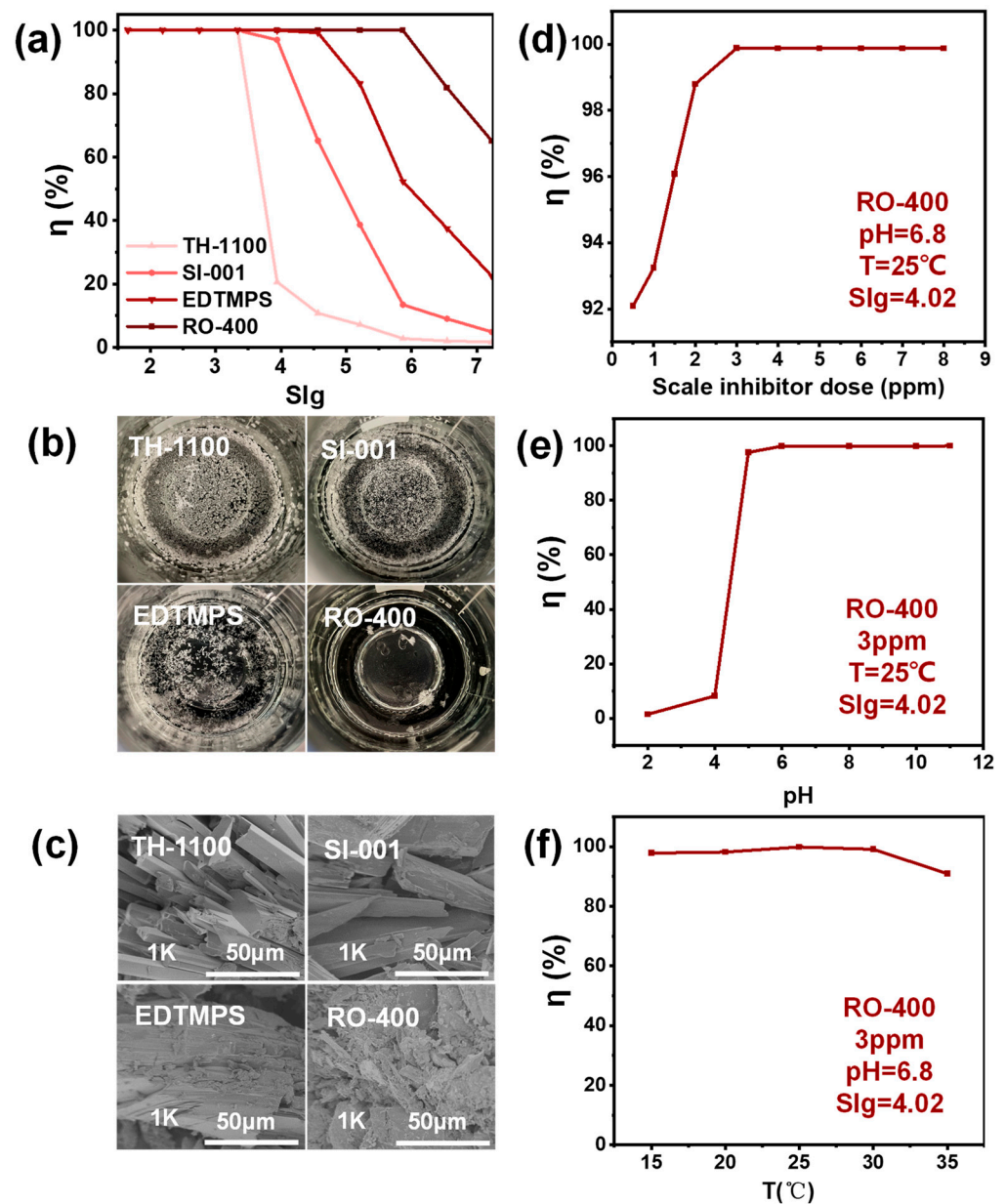


Figure 3. (a) The inhibition performance of different scale inhibitors in simulated concentrates; (b) digital photographs; and (c) SEM images of scaling materials after 10 h with different scale inhibitors (SIg = 6.5). The effect of (d) dose, (e) pH, and (f) temperature on the inhibition performance of RO-400.

Figure 4b shows an SEM image of CaSO_4 precipitation at $t = 35$ min of the UVD-GSP processes. With the increase in UV intensity in the UVD stage, the crystal structure of CaSO_4 in the GSP process is more complete, indicating the more significant degradation of the scale inhibitor. At a fixed dose of H_2O_2 , the increase in UV intensity can increase the concentration of hydroxyl radicals in the concentrate, leading to the improved degradation of scale inhibitors in the UVD process [34].

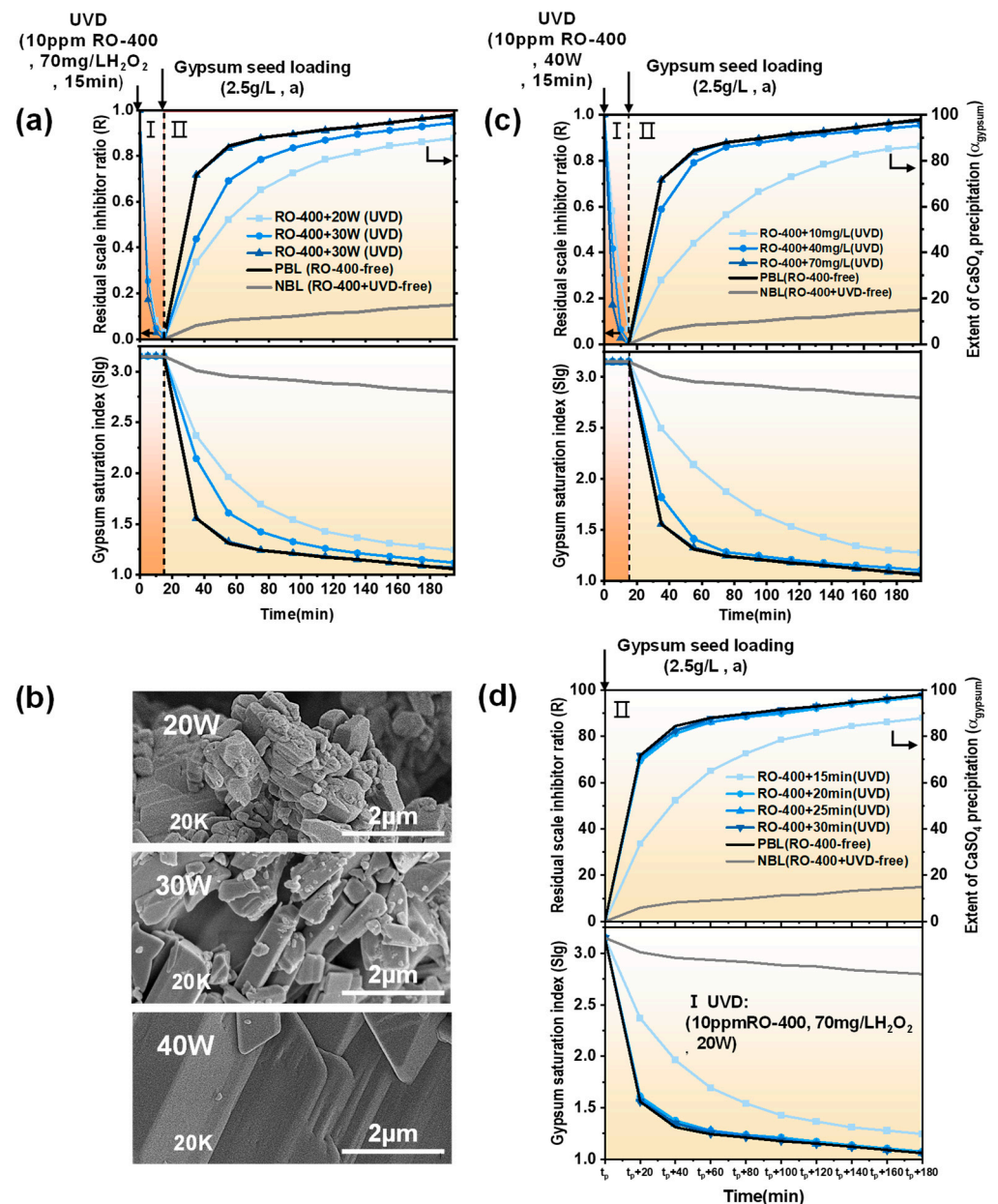


Figure 4. The effect of (a) UV intensity, (c) H_2O_2 dose, and (d) t_p on the residual scale inhibitor ratio (R) in UVD. (b) SEM images of CaSO_4 in the subsequent GSP process using different UV intensities in UVD ($t = 35$ min).

Figure 4c illustrates the effect of H_2O_2 dose on the performance of UVD-GSP. At the UVD stage, 10 mg/L H_2O_2 is added to the model concentrate B-bulk. After 15 min of irradiation under a 40 W UV light, 7% of the scale inhibitor remains (Table S1). Then, 2.5 g/L (7–43 μm) of crystal seeds is added. After the 180-min GSP desaturation process, the precipitation degree of CaSO_4 reaches 86.24%, and the SIg is reduced to 1.28, which is still far from the curve of PBL. When the H_2O_2 dose increases from 10 mg/L to 70 mg/L, the scale inhibitor content is reduced from 7% to 0% after the UVD stage (Table S1). In the subsequent GSP process, the precipitation degree of CaSO_4 and the SIg gradually approach the PBL baseline. This is due to the fact that the concentration of hydroxyl radicals in the concentrated solution is determined by the dose of H_2O_2 . Increasing the dose of H_2O_2 will increase the concentration of hydroxyl radicals and enhance the degradation of scale inhibitors.

Figure 4d presents the effect of light pretreatment time (t_p) on the UVD-GSP processes. In the UVD stage, 70 mg/L H_2O_2 is added, and 3% of the scale inhibitor remains after 15 min of irradiation with a 20 W UV light (Table S1). Subsequently, after the 180-min GSP desaturation process (adding 2.5 g/L, 7–43 μ m seeds), the precipitation degree of $CaSO_4$ only reaches 87.8% and the SIg is 1.25, which deviates from the baseline PBL seriously. The residual scale inhibitor is completely removed by extending the UVD pretreatment time from 15 min to 20 min, where the precipitation degree of $CaSO_4$ reaches 97.12%, and the SIg is reduced to 1.07. This indicates that the oxidative degradation of scale inhibitors by hydroxyl radicals in UVD requires a certain amount of time, and prolonged UV light treatment time can increase the extent of scale inhibitor degradation, thus reducing the inhibitory effect in the GSP process [34].

As shown above in Figure 4a, in the model concentrate B-bulk with 70 mg/L H_2O_2 , 3% of the scale inhibitor remains after 20 W UV irradiation for 15 min (Table S1). We fixed this UVD operating condition and explored the effects of seed particle size and loading amount on the GSP process.

In Figure 5a, after the 180-min GSP process, with the increase in seed particle size, the precipitation degree of $CaSO_4$ decreases from 87.8% to 77.98%, and the SIg increases from 1.25 to 1.43. That is, under the same seed loading, the larger the seed particle size, the worse the desaturation of $CaSO_4$. This is because the seed particles with a larger size provide a smaller active surface for slower $CaSO_4$ precipitation [35].

In Figure 5b, when the seed loading increases from 1.5 g/L to 5.5 g/L (7–43 μ m), the precipitation degree of $CaSO_4$ increases from 70.86% to 94.58%, and the SIg decreases from 1.56 to 1.12 after the 180-min GSP process. This is because the increase in seed loading can provide a more active surface for the growth of $CaSO_4$ crystals, overcoming the blocking effect of residual scale inhibitors and accelerating the kinetic process for the formation of $CaSO_4$ precipitation [35].

In addition, we also investigated the reusability of the seeds. The parameters of 2.5 g/L seeds with a size of 7–43 μ m are used for the GSP cycle experiments. In order to eliminate the adverse effects of residual scale inhibitors, GSP cycle experiments were carried out after UVD without scale inhibitor residues (40 W, 70 mg/L, 15 min). In Figure 5c, after adding the initial seeds, the kinetic curve is almost coincident with the PBL baseline. In the first cycle, the kinetic curve has a slight deviation from the PBL baseline. In the third cycle, the precipitation degree of $CaSO_4$ in the GSP process is 91.53%, and the SIg reaches 1.18, suggesting the seed cycle performance is satisfactory.

Figure 5d shows the particle size distribution of the recycled seeds. It can be seen that the particle size distribution of the seeds gradually migrates to larger sizes after the cycle experiments. In Figure 5e, after three cycles of GSP experiments, the surface of the seeds is still smooth, and the morphology of the seeds has not changed much from the initial seeds. However, the seed particle size becomes larger after recycling.

In summary, during the UVD process, the optimal parameters are a 40 W ultraviolet lamp and 70 mg/L H_2O_2 with 15 min illumination, and there is no residual scale inhibitor under this operating condition. However, taking cost into account, the best UVD operating conditions are a 40 W UV lamp and 40 mg/L H_2O_2 with 15 min illumination. Under the above operating conditions, although there is a trace amount of scale inhibitor residue (1%), the precipitation degree of $CaSO_4$ (95.43%) and the SIg (1.10) after the 180-min GSP process are generally close to the PBL baseline.

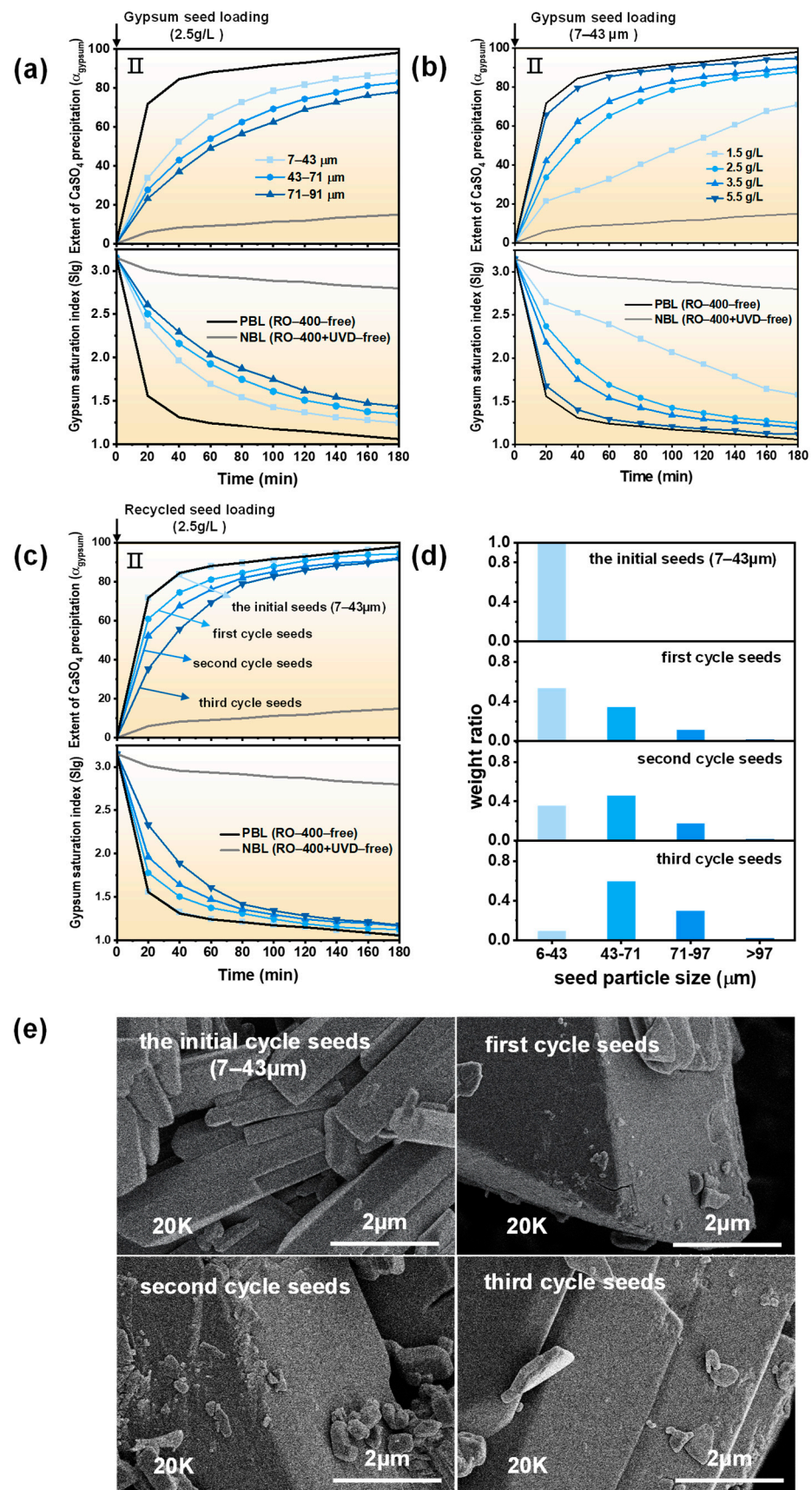


Figure 5. The effect of (a) seed particle size, (b) loading amount, and (c) recyclability of the seeds on the GSP process. (d) Particle size distribution and (e) SEM images of crystalline seeds added in each set of GSP for seed cycling experiments.

3. Experiment

3.1. Materials and Solutions

3.1.1. Materials

NaCl (99.5%) and $\text{CaSO}_4 \cdot 2\text{H}_2\text{O}$ (98%) were acquired from Tianjin Heowns Biochemical Technology Co., Ltd. Na_2SO_4 (99%), CaCl_2 (96%), H_2O_2 (30%), HCl (36%–38%), and NaOH (96%) were purchased from Tianjin Jiang Tian Chemical Technology Co., Ltd. Three different particle sizes of $\text{CaSO}_4 \cdot 2\text{H}_2\text{O}$ crystal seeds, 7–43 μm , 43–71 μm , and 71–91 μm , were obtained by sieving. All the reagents were used directly without further purification. Solutions were prepared using deionized water.

3.1.2. Scale Inhibitors

Currently, the scale inhibitors widely used in RO mainly include two types, one is phosphonate-based and the other is acrylic acid-based [30]. The commercial scale inhibitors used in this study consisted of two organophosphines and two polymers, 2-phosphonobutane-1,2,4-tricarboxylic acid (SI-001, Polymer Technology) (Figure 6a), ethylene diamine tetra methylene phosphonic acid sodium (EDTMPS, Shandong Taihe Technologies Co., Ltd.) (Figure 6b), low-molecular-weight polyacrylic acid partially neutralized salts (TH-1100, Shandong Taihe Technologies Co., Ltd.) (Figure 6c), and low-molecular-weight polyacrylic acid homopolymer (RO-400, BASF SE) (Figure 6d).

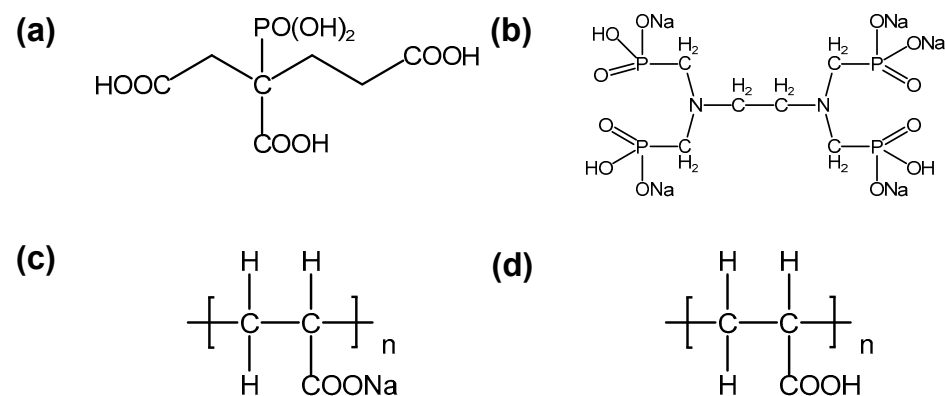


Figure 6. Chemical structure of the main components including (a) SI-001, (b) EDTMPS, (c) TH-1100, and (d) RO-400.

3.1.3. Preparation of RO Concentrate

The composition of the PRO concentrate model solution (A) is shown in Table 1. ESNA1-LF2-LD of FilmTec RO membrane modules from DOW were included in the case studies. The software IMSDesign (Version 2.229.87%) was used to calculate the bulk concentration (solution B-bulk) and the membrane surface concentration (solution B-membrane surface) when the SRO water recovery was 70% [15]. The specific composition is shown in Table 1.

Table 1. SRO concentrate model solutions for a coal chemical PRO concentrate at a 70% recovery rate.

Salt	PRO Concentrate Model Solution (A)		SRO Concentrate Model Solutions (70%)	
		Composition	Solution (B-Bulk)	Solution (B-Membrane Surface)
CaCl_2	mmol/L	12.85	42.91	52.22
Na_2SO_4	mmol/L	20.75	69.31	84.34
NaCl	mmol/L	26.40	88.20	107.33
pH	-	6.7	6.8	6.9
Slg	-	0.70	3.15	4.02

3.2. Experimental Details

3.2.1. Static Scale Inhibition Experiments

Static scale inhibition experiments were carried out according to GB/T 16632-2019 [36,37]. Specifically, simulated concentrated solutions of different SIg values were prepared, and the compositions are shown in Table S2. First, 8 ppm of TH-1100, SI-001, EDTMPS, or RO-400 was added to the simulated concentrated solution, stirred at a constant temperature for 10 h, and then filtered with a 0.22 μm disposable filter. The content of Ca^{2+} in the filtrate was determined by EDTA complexometric titration [38]. After selecting the appropriate scale inhibitor, the operating conditions including scale inhibitor dose, pH, and temperature were optimized using the model concentrate solution of B-membrane surface (Table 1).

The effectiveness of the scale inhibitor was evaluated by the scale inhibition efficiency (η , %), which was calculated according to the following equation,

$$\eta = \frac{c_2 - c_1}{c_0 - c_1} \quad (1)$$

where c_0 (mmol/L) represents the initial concentration of Ca^{2+} , c_1 (mmol/L) indicates the concentration of Ca^{2+} in the filtrate of the samples without the scale inhibitor, and c_2 (mmol/L) stands for the concentration of Ca^{2+} in the filtrate of the samples with the scale inhibitor.

3.2.2. UVD-GSP Experiments

ICD consists of two consecutive steps, UVD and GSP. For UVD, a certain amount of H_2O_2 was added to the prepared 1 L model concentrate B-bulk (10 ppm of RO-400) and irradiated under ultraviolet light for a certain time. The effects of light intensity, H_2O_2 dose, and light pretreatment time (t_p) on the UVD stage were investigated. Then, gypsum seeds were added to the model concentrate B-bulk after UV irradiation to realize the GSP process. The effects of seed particle size, loading amount, and recyclability of the seeds on GSP were explored.

During the experiments for UVD, 20 mL of samples were taken from the reactor at intervals of 5 min to measure the scale inhibitor content. The concentration of RO-400 in water samples was determined according to the turbidity method [39]. The absorbance was measured at a 420 nm wavelength, and the concentration of RO-400 was calculated according to the standard curve (Figure S2). The residual scale inhibitor ratio (R) was calculated according to the following equation,

$$R = \frac{c_{As,0} - c_{As}}{c_{As}} \quad (2)$$

where $c_{As,0}$ (ppm) and c_{As} (ppm) refer to the initial and sampling concentrations of the scale inhibitor in model concentrate B, respectively.

During the experiments for GSP, 3 mL of samples were taken from the reactor every 20 min, and the content of Ca^{2+} in the filtrate was measured after filtration. The pH change in solution B-bulk was monitored by pH meter. The saturation index of gypsum (SIg) was calculated by the software IMS Design [8]. The equation was as follows,

$$SIg = IAP/K_{sp, \text{gypsum}} \quad (3)$$

where IAP is the product of ion activity and $K_{sp, \text{gypsum}}$ is the solubility product of calcium sulfate.

The reaction degree of CaSO_4 (α_{gypsum}) was determined by the following formula [21],

$$\alpha_{\text{gypsum}} = \frac{c_0 - c}{c_0 - c_{eq}} \quad (4)$$

where c_{eq} represents the concentration of Ca^{2+} in solution B when $\text{CaSO}_4 \cdot 2\text{H}_2\text{O}$ is in equilibrium (Figure S3).

The morphology of gypsum seeds was characterized by scanning electron microscopy (SEM, Regulus 8100) at 3.0 kV. The particle size distribution of the crystalline seeds used in the cycling experiments was determined by employing shock sieving and weighed.

4. Conclusions

To improve the water recovery rate, a two-stage RO process with ICD is proposed to treat RO concentrates with a high CaSO_4 content. To avoid the scaling of the membrane surface during the SRO operation, scale inhibitors are added into the concentrates. After SRO, the scale inhibitor is destroyed by UV/ H_2O_2 degradation, and the resulting concentrate can be treated by the gypsum seeded precipitation (GSP) process.

For concentrates containing high CaSO_4 , suitable scale inhibitors were selected from the following three aspects: Ca^{2+} concentration in the concentrate, macroscopic scaling amount, and microscopic CaSO_4 precipitation morphology. RO-400, being the preferred scale inhibitor, shows an effective inhibition effect across a wide range of SIg (2.3–6) and pH (5–11) values. In the UVD process, a 40 W UV light with 70 mg/L H_2O_2 can degrade RO-400 completely in 15 min. In the GSP process, 2.5 g/L seeds with a size of 7–43 μm can decrease the SIg value to 1.07 (approaching the thermodynamic limit of 1) and remove 97% CaSO_4 . Gypsum seeds for the GSP process can be reused three times when there is no scale inhibitor residue in the UVD stage. This paper provides a clean and highly efficient method based on UV/ H_2O_2 to remove scale inhibitors from RO concentrates without the introduction of impurities to the entire system. The whole process studied to treat the concentrated solution containing high calcium sulfate by SRO, including scale inhibitor selection, degradation, and seed precipitation, can also provide guidance for actual production. Future work will focus on the applicability of the UVD-GSP-based RO treatment for water recovery and concentrate minimization in the desalination of CaSO_4 brines.

Supplementary Materials: The following supporting information can be downloaded at: <https://www.mdpi.com/article/10.3390/molecules29102163/s1>, Table S1: Ratio of the residual scale inhibitor (R) after the UVD stage for different operating conditions; Table S2: Composition of model concentrates with different gypsum saturation indices; Figure S1: SEM images of scaling materials after 10 h without scale inhibitor (SIg = 6.5); Figure S2. The standard curve of RO-400 concentration; Figure S3: Scale inhibitor-free calcium sulfate model solution C-bulk actual precipitation process ($c_{3 \text{ day}}$ considered as c_{eq}).

Author Contributions: Conceptualization, P.W., L.X. and W.Z.; methodology, S.X., P.W., Y.D. and W.Z.; investigation, S.X. and P.W.; software, Y.D.; validation, P.W. and Y.D.; formal analysis, P.W. and W.Z.; writing—original draft, P.W.; writing—review and editing, W.Z.; visualization, P.W. and W.Z.; supervision, S.X., L.X. and W.Z.; project administration, L.X.; funding acquisition, L.X. All authors have read and agreed to the published version of the manuscript.

Funding: This research was funded by the Hebei Provincial Central Leading Local Science and Technology Development Fund Project (226Z3101G) and the Hebei Provincial Natural Science Foundation (B2022202061).

Data Availability Statement: Data are contained within the article and Supplementary Materials.

Conflicts of Interest: The authors declare no conflicts of interest.

References

1. Xie, L.; He, X.; Liu, Y.; Cao, C.; Zhang, W. Treatment of reverse osmosis membrane by sodium hypochlorite and alcohols for enhanced performance using the swelling-fastening effect. *Chemosphere* **2022**, *292*, 133444. [[CrossRef](#)] [[PubMed](#)]
2. Xie, L.; Liu, Y.; Xu, S.; Zhang, W. Enhanced Anti-Biofouling Properties of BWRO Membranes via the Deposition of Poly (Catechol/Polyamine) and Ag Nanoparticles. *Membranes* **2023**, *13*, 530. [[CrossRef](#)] [[PubMed](#)]
3. Xu, S.; Zhao, H.; Xie, L.; Wang, K.; Zhang, W. Study on the Treatment of Refined Sugar Wastewater by Electrodialysis Coupled with Upflow Anaerobic Sludge Blanket and Membrane Bioreactor. *Membranes* **2023**, *13*, 527. [[CrossRef](#)] [[PubMed](#)]

4. Giwa, A.; Dufour, V.; Al Marzooqi, F.; Al Kaabi, M.; Hasan, S.W. Brine management methods: Recent innovations and current status. *Desalination* **2017**, *407*, 1–23. [[CrossRef](#)]
5. Shah, K.M.; Billinge, I.H.; Chen, X.; Fan, H.; Huang, Y.; Winton, R.K.; Yip, N.Y. Drivers, challenges, and emerging technologies for desalination of high-salinity brines: A critical review. *Desalination* **2022**, *538*, 115827. [[CrossRef](#)]
6. Li, X.; Hasson, D.; Semiat, R.; Shemer, H. Intermediate concentrate demineralization techniques for enhanced brackish water reverse osmosis water recovery—A review. *Desalination* **2019**, *466*, 24–35. [[CrossRef](#)]
7. Choi, J.Y.; Kaufmann, F.; Rahardianto, A.; Cohen, Y. Desupersaturation of RO concentrate and gypsum removal via seeded precipitation in a fluidized bed crystallizer. *Water Res.* **2021**, *190*, 116766. [[CrossRef](#)]
8. Gabelich, C.J.; Williams, M.D.; Rahardianto, A.; Franklin, J.C.; Cohen, Y. High-recovery reverse osmosis desalination using intermediate chemical demineralization. *J. Membr. Sci.* **2007**, *301*, 131–141. [[CrossRef](#)]
9. Chan, S.-S.; Wu, J.-H. Municipal-to-Industrial Water Reuse via Multi-Stage and Multi-Pass Reverse Osmosis Systems: A Step from Water Scarcity towards Sustainable Development. *Water* **2022**, *14*, 362. [[CrossRef](#)]
10. Miyakawa, H.; Maghram Al Shaihae, M.; Green, T.N.; Ito, Y.; Sugawara, Y.; Onishi, M.; Fusaoka, Y.; Farooque Ayumantakath, M.; Saleh Al Amoudi, A. Reliable Sea Water Ro Operation with High Water Recovery and No-Chlorine/No-Sbs Dosing in Arabian Gulf, Saudi Arabia. *Membranes* **2021**, *11*, 141. [[CrossRef](#)]
11. Penteado de Almeida, J.; Stoll, Z.; Xu, P. An Alternating, Current-Induced Electromagnetic Field for Membrane Fouling and Scaling Control during Desalination of Secondary Effluent from Municipal Wastewater. *Water* **2023**, *15*, 2234. [[CrossRef](#)]
12. Prisciandaro, M.; Innocenzi, V.; Tortora, F.; Mazziotti di Celso, G. Reduction of Fouling and Scaling by Calcium Ions on an UF Membrane Surface for an Enhanced Water Pre-Treatment. *Water* **2019**, *11*, 984. [[CrossRef](#)]
13. Xiong, R.; Chen, Q.; Liu, J.; Wei, C. Experimental study on seeded precipitation assisted reverse osmosis for industrial wastewater reuse. *J. Water Process Eng.* **2017**, *20*, 78–83. [[CrossRef](#)]
14. Prakash, N.; Chaudhuri, A.; Das, S.P. Numerical modelling and analysis of concentration polarization and scaling of gypsum over RO membrane during seawater desalination. *Chem. Eng. Res. Des.* **2023**, *190*, 497–507. [[CrossRef](#)]
15. Hydranautics. Chemical Pretreatment for RO and NF. In *Technical Application Bulletin No 111*; Hydranautics: Oceanside, CA, USA, 2013.
16. Chuan Yee Lee, B.; Tan, E.; Lu, Y.; Komori, H.; Pietsch, S.; Goodlett, R.; James, M. Antiscalant and its deactivation in zero/minimized liquid discharge (ZLD/MLD) application in the mining sector—Opportunities, challenges and prospective. *Miner. Eng.* **2023**, *201*, 108238. [[CrossRef](#)]
17. Greenlee, L.F.; Testa, F.; Lawler, D.F.; Freeman, B.D.; Moulin, P. The effect of antiscalant addition on calcium carbonate precipitation for a simplified synthetic brackish water reverse osmosis concentrate. *Water Res.* **2010**, *44*, 2957–2969. [[CrossRef](#)]
18. Rahman, F. Calcium sulfate precipitation studies with scale inhibitors for reverse osmosis desalination. *Desalination* **2013**, *319*, 79–84. [[CrossRef](#)]
19. Kum, S.; Tang, X.; Liu, H. Treatment of brackish water inland desalination brine via antiscalant removal using persulfate photolysis. *Environ. Sci.: Water Res. Technol.* **2023**, *9*, 1137–1146. [[CrossRef](#)]
20. McCool, B.C.; Rahardianto, A.; Cohen, Y. Antiscalant removal in accelerated desupersaturation of RO concentrate via chemically-enhanced seeded precipitation (CESP). *Water Res.* **2012**, *46*, 4261–4271. [[CrossRef](#)]
21. Rahardianto, A.; McCool, B.C.; Cohen, Y. Accelerated desupersaturation of reverse osmosis concentrate by chemically-enhanced seeded precipitation. *Desalination* **2010**, *264*, 256–267. [[CrossRef](#)]
22. Yang, Q.; Lisitsin, D.; Liu, Y.; David, H.; Semiat, R. Desupersaturation of RO Concentrates by Addition of Coagulant and Surfactant. *J. Chem. Eng. Jpn.* **2007**, *40*, 730–735. [[CrossRef](#)]
23. Halleb, A.; Nakajima, M.; Yokoyama, F.; Neves, M.A. Effect of Surfactants on Reverse Osmosis Membrane Performance. *Separations* **2023**, *10*, 168. [[CrossRef](#)]
24. Sun, S.; Zhao, Z.; Cui, X.; Huo, M.; Geng, Z. The Influence of Residual Coagulant Al on the Biofilm EPS and Membrane Fouling Potential in Wastewater Reclamation. *Water* **2020**, *12*, 1056. [[CrossRef](#)]
25. Khan, I.; Saeed, K.; Zekker, I.; Zhang, B.; Hendi, A.H.; Ahmad, A.; Ahmad, S.; Zada, N.; Ahmad, H.; Shah, L.A.; et al. Review on Methylene Blue: Its Properties, Uses, Toxicity and Photodegradation. *Water* **2022**, *14*, 242. [[CrossRef](#)]
26. Marszałek, A.; Puszczalo, E. Effect of Photooxidation on Nanofiltration Membrane Fouling During Wastewater Treatment from the Confectionery Industry. *Water* **2020**, *12*, 793. [[CrossRef](#)]
27. Ali, M.A.; Maafa, I.M.; Qudsieh, I.Y. Photodegradation of Methylene Blue Using a UV/H₂O₂ Irradiation System. *Water* **2024**, *16*, 453. [[CrossRef](#)]
28. He, X.; Pelaez, M.; Westrick, J.A.; O’Shea, K.E.; Hiskia, A.; Triantis, T.; Kaloudis, T.; Stefan, M.I.; de la Cruz, A.A.; Dionysiou, D.D. Efficient removal of microcystin-LR by UV-C/H₂O₂ in synthetic and natural water samples. *Water Res.* **2012**, *46*, 1501–1510. [[CrossRef](#)]
29. Yuan, H.; Zhang, Y.; Zhou, X. Degradation of Bezafibrate with UV/H₂O₂ in Surface Water and Wastewater Treatment Plant Effluent. *CLEAN Soil Air Water* **2011**, *40*, 239–245. [[CrossRef](#)]
30. Yu, W.; Song, D.; Chen, W.; Yang, H. Antiscalants in RO membrane scaling control. *Water Res.* **2020**, *183*, 115985. [[CrossRef](#)]
31. Gu, X.; Qiu, F.; Zhou, X.; Qi, J.; Zhou, Y.; Yang, D.; Guo, Q.; Guo, X. Synthesis and application of terpolymer scale inhibitor in the presence of β -cyclodextrins. *J. Pet. Sci. Eng.* **2013**, *109*, 177–186. [[CrossRef](#)]

32. Greenlee, L.F.; Testa, F.; Lawler, D.F.; Freeman, B.D.; Moulin, P. Effect of antiscalants on precipitation of an RO concentrate: Metals precipitated and particle characteristics for several water compositions. *Water Res.* **2010**, *44*, 2672–2684. [[CrossRef](#)]
33. Chen, J.; Xu, L.; Han, J.; Su, M.; Wu, Q. Synthesis of modified polyaspartic acid and evaluation of its scale inhibition and dispersion capacity. *Desalination* **2015**, *358*, 42–48. [[CrossRef](#)]
34. Zhang, Y.; Zhou, L.; Zhang, Y.; Tan, C. Inactivation of *Bacillus subtilis* spores using various combinations of ultraviolet treatment with addition of hydrogen peroxide. *Photochem. Photobiol.* **2014**, *90*, 609–614. [[CrossRef](#)]
35. Zhang, H.; Kou, J.; Sun, C. Combing Seeding Crystallization with Flotation for Recovery of Fluorine from Wastewater: Experimental and Molecular Simulation Studies. *Molecules* **2023**, *28*, 4490. [[CrossRef](#)]
36. Yu, W.; Wang, Y.; Li, A.; Yang, H. Evaluation of the structural morphology of starch-graft-poly(acrylic acid) on its scale-inhibition efficiency. *Water Res.* **2018**, *141*, 86–95. [[CrossRef](#)]
37. Zhang, S.; Qu, H.; Yang, Z.; Fu, C.-e.; Tian, Z.; Yang, W. Scale inhibition performance and mechanism of sulfamic/amino acids modified polyaspartic acid against calcium sulfate. *Desalination* **2017**, *419*, 152–159. [[CrossRef](#)]
38. Kimaru, I.W.; Corigliano, A.T.; Zhao, F. Using Classical EDTA Titrations To Measure Calcium and Magnesium in Intravenous Fluid Bags. *J. Chem. Educ.* **2018**, *95*, 2238–2242. [[CrossRef](#)]
39. Mkrtchyan, K.V.; Pigareva, V.A.; Zezina, E.A.; Kuznetsova, O.A.; Semenova, A.A.; Yushina, Y.K.; Tolordava, E.R.; Grudistova, M.A.; Sybachin, A.V.; Klimov, D.I.; et al. Preparation of Biocidal Nanocomposites in X-ray Irradiated Interpolyelectolyte Complexes of Polyacrylic Acid and Polyethylenimine with Ag-Ions. *Polymers* **2022**, *14*, 4417. [[CrossRef](#)]

Disclaimer/Publisher’s Note: The statements, opinions and data contained in all publications are solely those of the individual author(s) and contributor(s) and not of MDPI and/or the editor(s). MDPI and/or the editor(s) disclaim responsibility for any injury to people or property resulting from any ideas, methods, instructions or products referred to in the content.